Overcoming the Bottleneck of the Enzymatic Cycle by Steric Frustration

Wenfei Li,[1,*] Jun Wang,[1] Jian Zhang,[1] Shoji Takada,[2,†] and Wei Wang[1,‡]
[1]*Department of Physics, National Laboratory of Solid State Microstructure, and Collaborative Innovation Center of Advanced Microstructures, Nanjing University, Nanjing 210093, China*
[2]*Department of Biophysics, Graduate School of Science, Kyoto University, Kyoto 606-8502, Japan*

(Received 10 January 2019; revised manuscript received 10 April 2019; published 14 June 2019)

The enormous catalytic power of natural enzymes relies on the ability to overcome the bottleneck event in the enzymatic cycle, yet the underlying physical mechanisms are not fully understood. Here, by performing molecular simulations of the whole enzymatic cycle for a model multisubstrate enzyme with a dynamic energy landscape model, we show that multisubstrate enzymes can utilize steric frustration to facilitate the rate-limiting product-release step. During the enzymatic cycles, the bottleneck product is actively squeezed out by the binding of a new substrate at the neighboring site through the population of a substrate-product cobound complex, in which the binding pockets are frustrated due to steric incompatibility. Such steric frustration thereby enables an active mechanism of product release driven by substrate-binding energy, facilitating the enzymatic cycle.

DOI: 10.1103/PhysRevLett.122.238102

Natural enzymes have evolved to catalyze biochemical reactions with high efficiency by coordinating the substrate-binding, chemical-reaction, and product-release steps in enzymatic cycle [1]. For enzymes with a sufficiently fast chemical reaction step [2], the overall enzymatic rate is often limited by the ability to undergo substrate-product exchange, particularly the product-release step, which is coupled with conformational motions [2–6]. Slow product-release tends to hinder the uptake of new substrate, and therefore the overall cycle, giving rise to product inhibition effect. Revealing the strategies natural enzymes use to facilitate the rate-limiting step in an enzymatic cycle is the key to understanding their enormous catalytic power. Recent advancements in single-molecule techniques and high-resolution spectroscopy are making it possible to directly probe various aspects of enzymatic cycle [5–8], which promoted a number of elegant experimental and theoretical studies to address the physics basis of enzyme catalysis [6–22].

Although most enzyme models were derived for single-substrate enzymes [1], enzymatic reactions involving multiple substrates and products are more common. In the enzymatic cycle of these multisubstrate enzymes, the substrate-product exchange (i.e., product release and new substrate binding) may encounter multiple intermediate binding states and pathways, which makes the elucidation of the enzymatic mechanism extremely challenging, and different mechanisms have been proposed [1,23]. For example, even in the bisubstrate-biproduct reactions, which account for more than 60% of the known enzymatic reactions and often involve the transfer of a chemical group from one substrate to another, maximally nine binding states (hereafter referred to as chemical states) can be populated during the cycle (Fig. 1). Moreover, there exist pathways in which the new substrate binds to one site before the release of the product at the neighboring site, leading to populations of hybrid complexes, with substrate

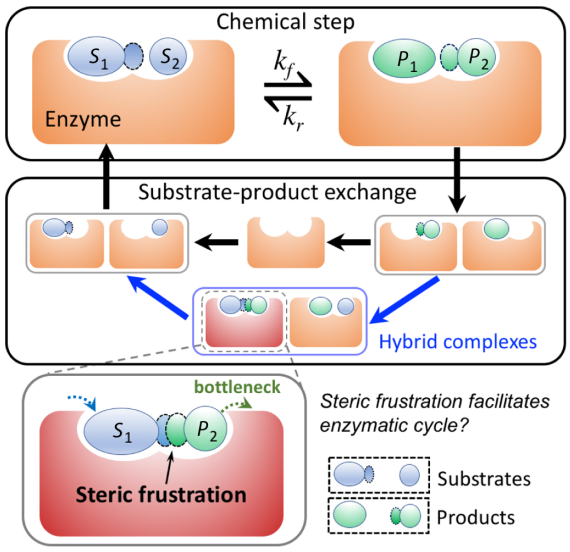

FIG. 1. Schematic of the enzymatic cycle of a bisubstrate-biproduct reaction $S_1 + S_2 \rightleftharpoons P_1 + P_2$, which catalyzes the transfer of a chemical group (dashed ellipse) from one substrate (S_1) to another (S_2), producing two products (P_1 and P_2). Because each binding site can be substrate bound, product bound, or empty, the substrate-product exchange maximally encounters nine chemical states, including two hybrid complexes with substrate and product cobound at the neighboring sites. In the hybrid complex S_1P_2 (red), the substrate S_1 and product P_2 are sterically incompatible due to the overlap of the two transferring groups, leading to steric frustration in the binding pockets.

and product cobound. Particularly, in one hybrid complex (Fig. 1, bottom), due to the presence of an extra chemical group, the binding sites cannot precisely accommodate the cobound substrate and product, leading to steric frustration by competitive interactions in the pockets. Although it was often assumed that these hybrid states correspond to dead-end complexes and do not contribute to productive catalysis [1], it is natural to imagine that the frustration also tends to cause destabilization of the otherwise tightly bound product, and thereby speeding up the bottleneck product release in an enzymatic cycle. However, the actual role of such direct substrate-product interplay on the enzymatic activity remains elusive. In addition, large-amplitude conformational motions can be crucial for the enzymatic cycle because the substrate-product exchange and chemical reaction preferably occur at the conformations with exposed and closed binding pockets, respectively [5,6]. How natural multisubstrate enzymes coordinate these tightly coupled events in the cycle to facilitate the rate-limiting step remains poorly understood, partly due to the difficulty to achieve a whole enzymatic-cycle characterization in experiments.

In this Letter, we introduce a new enzyme model at residue resolution based on a dynamic energy landscape perspective [24]. Our model can provide whole enzymatic-cycle dynamics with considerations of direct substrate-product interplay and explicit conformation-activity coupling, buttressed by available experimental data. Applying to a model bisubstrate-biproduct enzyme, adenylate kinase (AdK) [25], not only reproduced the available experimental data of turnover kinetics [26], but also revealed an efficient strategy for multisubstrate enzymes to facilitate the rate-limiting step of enzymatic cycle. We showed that the enzyme utilizes steric frustration encountered in the substrate-product cobound complex to facilitate the rate-limiting release of the slow product (P_2, Fig. 1 bottom) by dynamic variation of the energy landscape and barrier lowering upon new substrate binding (S_1), enabling an active mechanism of product release and expedited enzymatic cycle.

Let us consider an enzyme that possesses n ligand-binding sites. We assume that the ith binding site takes discrete ligand states ls_i depending on the kinds of bound ligands. The energy function at a given chemical state $(ls_1, ls_2, ..., ls_n)$ is written as

$$V(\vec{x}, ls_1, ls_2, \ldots, ls_n) = V_{\mathrm{apo}}(\vec{x}) + \sum_{i=1}^{n} V^i_{\mathrm{bind}}(\vec{x}, ls_i), \qquad (1)$$

where $\vec{x}$ collectively represents the coordinates of residues. $V_{\mathrm{apo}}(\vec{x})$ is the energy function of the enzyme at the apo state dictating conformational motions by molecular dynamics (MD) simulations, and has a multibasin topography. Previous theoretical work showed that the specificity-activity correlation of enzymes can be well captured by the energy landscape topography [27]. $V^i_{\mathrm{bind}}(\vec{x}, ls_i)$ is the ligand binding energy of the binding pocket i, with ligand state ls_i. Therefore, variation of the chemical states, either by substrate-product exchange or by chemical reactions, reshapes the energy landscapes, leading to modified conformational motions during the cycle. We used the multibasin model and the implicit ligand binding potential developed in our previous work [28–30] for the terms $V_{\mathrm{apo}}(\vec{x})$ and $V^i_{\mathrm{bind}}(\vec{x}, ls_i)$, with the parameters determined by available experimental data and atomistic force field (see the Supplemental Material for details [31]). For the model enzyme AdK [Fig. 2(a) and Fig. S1], which catalyzes the phosphoryl transfer reaction $\mathrm{ATP} + \mathrm{AMP} \rightleftharpoons \mathrm{ADP} + \mathrm{ADP}$ and consists of three domains [the CORE domain, the LID domain that binds ATP(T) or ADP(D), and the NMP domain that binds AMP(M) or ADP)], the LID site takes $ls_1 = \mathrm{T}, \mathrm{D}$, or empty($\varnothing$), and the NMP site takes $ls_2 = \mathrm{M}, \mathrm{D}$, or $\varnothing$, leading to nine possible chemical states ($ls_1 ls_2$), therefore nine energy landscapes dictate the conformational motions. The energy functions allow for separate motions of the LID and NMP domains with high cooperativity (Figs. S2–S4), consistent with previous MD simulations [61,62]. The free energy landscape at apo state ($\varnothing\varnothing$) exhibits four major conformational states as a result of the opening or closing motions of the two lids [Fig. 2(c)]. Presence of substrates stabilizes the closed conformation (Fig. S3), which is in agreement with experimental data [5,6].

We thereby describe the enzymatic cycle as the conformational motions on the individual energy landscapes and the transitions between these energy landscapes due to substrate-product exchange and chemical reactions, as schematically drawn in Fig. 2(d) for AdK. The binding and dissociation of the substrate or product molecules are realized by a Metropolis Monte Carlo scheme with the rates depending on the substrate or product concentration, binding energy, and solvent accessible surface area (SASA) of the binding pockets. The substrate binding is assumed to be diffusion limited and occurs with the rate

$$k_{\mathrm{bind}} = f(S) k_{\mathrm{on}} [L], \qquad (2)$$

where k_{on}, $[L]$, and S are the second-order rate constant, substrate or product concentration, and SASA of the binding pocket, respectively. The $f(S) = 1.0/\{1 + \exp[-(S - S_0)/\sigma_S]\}$ describes the dependence of the ligand exchange rate on the geometry of the binding pocket [31]. The ligand dissociation follows the rate

$$k_{\mathrm{off}} = f(S) k_u^0 \exp[-V^i_{\mathrm{bind}}(\vec{x}, ls_i)/k_B T]. \qquad (3)$$

The chemical reaction step, i.e., the conversion between substrate and product, is described by a similar scheme with the forward (k_f) and reverse (k_r) reaction rates given by experimental data [31].

With the above dynamic energy landscape model of enzymatic dynamics, we then simulated the whole enzymatic

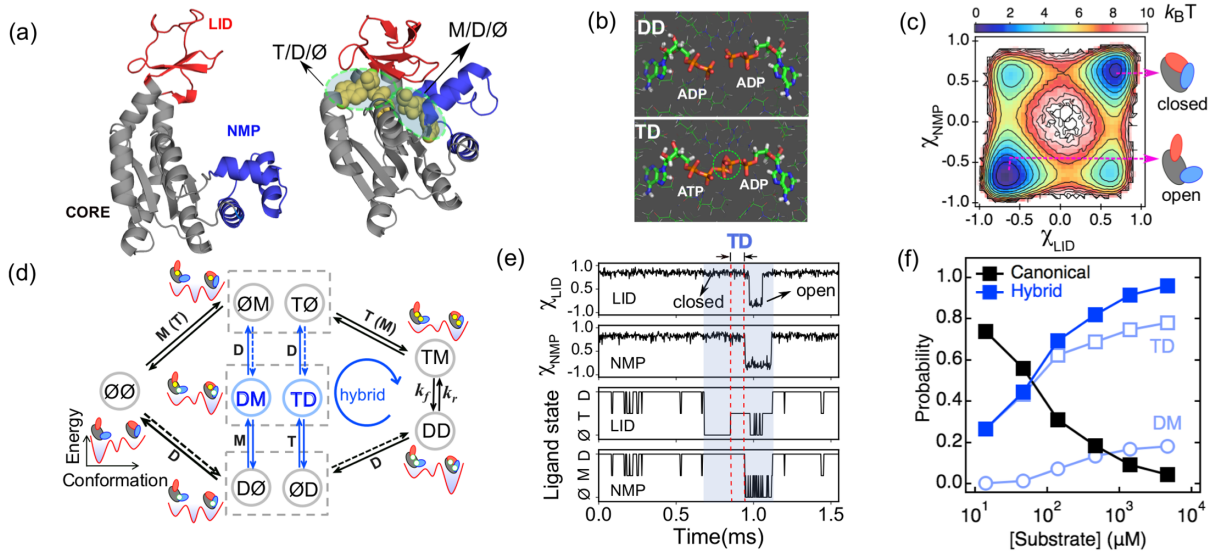

FIG. 2. Dynamic energy landscape model of enzyme catalysis. (a) Structures of AdK at open (inactive)—left—and closed (active)—right—conformations. (b) Structures of the bound ligands in the chemical states DD and TD. (c) Free energy landscape showing the conformational fluctuations of the two lids at apo state. The reaction coordinates χ_{LID} and χ_{NMP} take negative (positive) values in the open (closed) conformations [31]. (d) Schematic diagram showing the dynamic energy landscape model of the whole enzymatic-cycle of AdK, assuming a stepwise ligand exchange process. The transitions with dashed lines are prohibited without supplying ADP. The effects of substrate-product exchange on the energy landscapes were schematically shown for selected chemical states. (e) MD trajectory showing the conformational motions and ligand exchange for a representative enzymatic cycle at $[ATP] = [AMP] = 150\ \mu M$. The shaded region corresponds to the substrate-product exchange. (f) Relative probabilities of the canonical pathway (black) and hybrid pathway (blue) of the enzymatic cycle as a function of substrate concentration. The results of two subpathways via TD and DM are also shown.

cycle of AdK, for which the product release is the rate-limiting step [5,6]. Experimentally, the catalytic turnover rate is often measured under steady-state conditions [26]. Similarly, we conducted simulations of the enzymatic cycle with concentrations of the substrates ATP and AMP fixed to certain values and the concentration of the product ADP set to zero. This simulation resulted in stochastic dynamics with multiround enzymatic cycles coupled with conformational motions [Figs. 2(e) and S5]. We define the enzymatic cycle as one starting from and ending with ADP dissociation from the DD state, which contributes to one productive turnover event. From the prototypical time course of an enzymatic cycle shown in Fig. 2(e), one can see tight coupling between the conformational motions, substrate-product exchanges, and overall turnovers, implying the importance of integrated modeling of the whole enzymatic cycle.

From the simulated enzymatic cycles, we are able to extract the turnover kinetics, and the results can well reproduce the experimental data (Fig. S6). In addition, previous experimental study on AdK showed that the catalytic activity tends to be reduced when conformational equilibrium is biased to closed conformation by mutational and osmolyte-driven perturbations, which can be well reproduced by our simulations (Fig. S6) [26]. The success of the whole enzymatic-cycle model in describing the turnover kinetics and the conformation-activity interplay enables the in-depth characterization of the underlying enzymatic mechanism.

As schematically shown in Fig. 2(d), enzymatic cycle may follow two distinct pathways, including (i) canonical pathway, in which the substrate binding occurs after full dissociation of the two products (black arrows), and (ii) hybrid pathway, in which the enzymatic cycle involves the substrate-product cobound complexes (TD or DM) (blue-black arrows). In the TD state, e.g., the product ADP from the previous round remains in the NMP-domain pocket, while the substrate ATP for the next round binds to the LID domain [Fig. 2(e)]. Although the hybrid pathway is often not considered in the current paradigm of AdK catalysis, our simulation data showed that the two pathways can coexist, and both contribute to productive catalysis. For the forward reactions, the probability of the hybrid pathway increases with substrate concentrations and becomes dominant at high concentrations [Fig. 2(f)]. In this hybrid pathway, the subpathway via TD state has a much higher probability (~0.8). We note that the ATP concentration in the cell varies and can be as high as 10 mM [63], which includes the range investigated in this Letter.

The TD state is an intriguing state from a structural perspective. While the AdK structure accommodates the two products (substrates) favorably in the catalytically competent DD (TM) state, the terminal phosphate groups of the ATP and ADP sterically overlap in the TD state

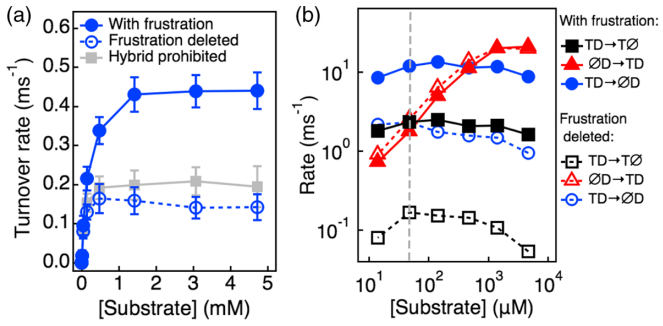

FIG. 3. Steric frustration facilitates the bottleneck step of enzymatic cycle. (a) Turnover rates versus substrate concentrations for the intact simulations (filled circles), control simulations with substrate-product coupling deleted in the TD state (open circles), and simulations with the hybrid pathway prohibited (squares). The error bars represent standard deviation of 20 independent simulations. (b) Rates of the key steps in the substrate-product exchange for the intact simulations (filled) and the control simulations (open).

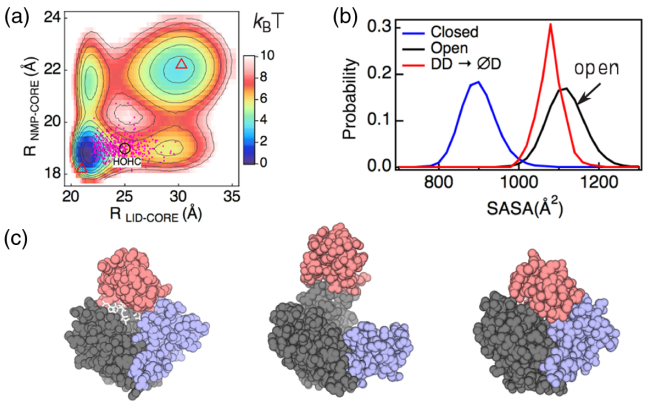

FIG. 4. Role of conformational plasticity on the substrate-product exchange. (a) Projection of the snapshots, at which the LID-domain ADP dissociates from the state DD (red dots), onto the free energy landscape constructed from all conformations. The substrate concentration is 150 μM. Black circle: center of the HOHC state in Ref. [22]; red triangles: crystal structures of the open and closed states. (b) Distributions of SASA for the ADP-releasing snapshots (red), together with the distributions of the closed (blue) and open (black) conformations. (c) A representative snapshot of partly open conformation taken from all-atom simulations with DD state (left). ADPs are colored white. Crystal structures of open (middle) and closed (right) conformations are also shown.

[circle in Fig. 2(b)]. Undoubtedly, this steric incompatibility tends to destabilize the binding of the two molecules mutually and therefore introduce frustration to the binding pockets. It is interesting to investigate how such steric frustration contributes to the overall catalysis. We compared the simulation results from this intact model (with steric frustration) with the results of control simulations in which the steric frustration effect was absent [Figs. 3(a) and S7] [31]. Surprisingly, this steric frustration between the ATP and ADP in the TD state makes a positive contribution to the overall catalysis, increasing the turnover rate by a factor of 3 at a wide range of concentrations. The resulted turnover rate is also much higher than that of the simulations with the hybrid pathway prohibited. Detailed analysis revealed that the steric frustration facilitates the enzymatic cycle by accelerating the bottleneck product ADP release [Fig. 3(b)], and the effect is insensitive to the conformation change pathways (Fig. S8) [62]. As expected, the steric frustration also slows down the productive ATP binding, which has an inhibitive effect on the catalysis. However, when the substrate concentration is higher than 50 μM, the substrate ATP binding is always faster than the bottleneck product ADP dissociation [Figs. 3(b) and S9]. Consequently, the effect of steric frustration on the product ADP release becomes dominant and enhances the turnover rate. The destabilization effect of the TD state on the closed conformation was also supported by atomistic MD simulations (Fig. S10).

As discussed above, the efficient catalysis relies on the population of the hybrid state TD, which requires the fast dissociation of the LID-domain ADP and uptaking of new substrate ATP. The simulation trajectories showed that starting from the postreaction state (i.e., chemical state DD), the LID-domain ADP tends to dissociate earlier (with probability of ~0.80). Interestingly, the release of this ADP occurs predominantly without fully opening the LID domain [Fig. 4(a), red dots]. However, the distribution of the SASA of the binding site for these ADP releasing snapshots is biased to that of the open state [Fig. 4(b), red], indicating that the binding pocket is plastic and can be largely exposed even without fully opening the LID domain. Such partly open conformation with an exposed binding pocket can be easily sampled in the all-atom MD simulations [Figs. 4(c) and S10]. Once the binding pocket is exposed, both the ADP release and new ATP binding become energetically easier, which increases the population of the TD hybrid complex and therefore speeds up the release of the slow ADP by steric frustration. Interestingly, previous MD simulations by Bagchi and co-workers suggested a half-open half-closed (HOHC) intermediate state [22], which was considered crucial for the enzymatic cycle. The partly open conformation revealed in this Letter is compatible with the HOHC state [Fig. 4(a), black circle]. Furthermore, the above results directly demonstrated the key role of such state in the enzymatic-cycle. The binding pocket plasticity is also consistent with a recent experimental work [64], which showed that the closed-like conformation is capable of substrate binding without occlusion by steric hindrance. Our simulations following the experimental setup well reproduced the experimental observation(Fig. S11), highlighting the importance of appropriate conformational plasticity.

The catalysis of bi-substrate enzymes was often described by the random sequential bi-bi mechanism [1,23]. Within

such a mechanism, catalysis will tend to be slowed down by the product inhibition effect because the ligand-binding sites can be occupied by products, which hinders the binding of new substrates. Notably, in our study, the product comes directly from catalysis and thus is a cis-product in contrast to the transproduct that rebinds from buffer. Natural enzymes must develop a certain strategy to overcome the challenge of product inhibition to realize efficient catalysis. Our results reveal that multisubstrate enzymes can utilize steric frustration to reduce product inhibition by populating a hybrid chemical state with steric incompatibility, in which the binding of a new substrate actively squeezes out the neighboring product, speeding up the bottleneck product-release event. Such effects are distinct from the ground state destabilization mechanism [65,66].

The crucial role of the steric frustration revealed in this Letter is somewhat counterintuitive, considering that it has been well established that the evolution of natural proteins tends to minimize the frustrations of physical interactions as required by protein folding [24]. However, accumulative evidence showed that the sites related to protein functions are often locally frustrated [67,68]. The findings in this Letter demonstrated, for the first time to our knowledge, that natural multisubstrate enzymes can utilize frustration between substrate and product molecules to facilitate catalysis. In addition, the steric frustration revealed in this Letter renders the product release an active process driven by substrate binding, which is in contrast to the passive mechanism based on binding affinities as implied in most enzyme models.

As the model enzyme discussed in this Letter shares the common features of most multisubstrate enzymes [31], the new strategies for achieving efficient catalysis revealed in this Letter may represent a general mechanism. With the rapid development of modern single-molecule enzymology techniques [7], it will be interesting in future studies to experimentally characterize the role of steric frustration in enzymatic cycle. In addition, the above dynamic energy landscape model of enzyme catalysis has been implemented based on the molecular simulation software CafeMol (www.cafemol.org) [69] and it can be readily applied to other enzymes with the input of some key parameters from experiments or high-level theoretical computations.

This work was supported by the National Natural Science Foundation of China (Grants No. 11574132, No. 11774157, and No. 11774158) and the HPC center of Nanjing University.

*wfli@nju.edu.cn
†takada@biophys.kyoto-u.ac.jp
‡wangwei@nju.edu.cn

[1] I. H. Segel, *Enzyme Kinetics* (Wiley, New York, 1993).
[2] E. D. Watt, H. Shimada, E. L. Kovrigin, and J. P. Loria, Proc. Natl. Acad. Sci. U.S.A. **104**, 11981 (2007).
[3] W. W. Cleland, Acc. Chem. Res. **8**, 145 (1975).
[4] S. J. Benkovic and S. Hammes-Schiffer, Science **301**, 1196 (2003).
[5] K. A. Henzler-Wildman, V. Thai, M. Lei, M. Ott, M. Wolf-Watz, T. Fenn, E. Pozharski, M. A. Wilson, G. A. Petsko, M. Karplus *et al.*, Nature (London) **450**, 838 (2007).
[6] J. A. Hanson, K. Duderstadt, L. P. Watkins, S. Bhattacharyya, J. Brokaw, J.-W. Chu, and H. Yang, Proc. Natl. Acad. Sci. U.S.A. **104**, 18055 (2007).
[7] H. P. Lu, Chem. Soc. Rev. **43**, 1118 (2014).
[8] H. G. Saavedra, J. O. Wrabl, J. A. Anderson, J. Li, and V. J. Hilser, Nature (London) **558**, 324 (2018).
[9] B. Pelz, G. Žoldák, F. Zeller, M. Zacharias, and M. Rief, Nat. Commun. **7**, 10848 (2016).
[10] S. J. Kerns, R. V. Agafonov, Y.-J. Cho, F. Pontiggia, R. Otten, D. V. Pachov, S. Kutter, L. A. Phung, P. N. Murphy, V. Thai *et al.*, Nat. Struct. Mol. Biol. **22**, 124 (2015).
[11] H. Y. Aviram, M. Pirchi, H. Mazal, Y. Barak, I. Riven, and G. Haran, Proc. Natl. Acad. Sci. U.S.A. **115**, 3243 (2018).
[12] A. Ariyaratne, C. Wu, C.-Y. Tseng, and G. Zocchi, Phys. Rev. Lett. **113**, 198101 (2014).
[13] H. Qu and G. Zocchi, Phys. Rev. X **3**, 011009 (2013).
[14] Q. Lu and J. Wang, J. Am. Chem. Soc. **130**, 4772 (2008).
[15] M. D. Daily, G. N. Phillips, and Q. Cui, J. Mol. Biol. **400**, 618 (2010).
[16] P. C. Whitford, O. Miyashita, Y. Levy, and J. N. Onuchic, J. Mol. Biol. **366**, 1661 (2007).
[17] M. B. Kubitzki and B. L. de Groot, Structure **16**, 1175 (2008).
[18] Y. Matsunaga, H. Fujisaki, T. Terada, T. Furuta, K. Moritsugu, and A. Kidera, PLoS Comput. Biol. **8**, e1002555 (2012).
[19] V. Casagrande, Y. Togashi, and A. S. Mikhailov, Phys. Rev. Lett. **99**, 048301 (2007).
[20] A. V. Pisliakov, J. Cao, S. C. Kamerlin, and A. Warshel, Proc. Natl. Acad. Sci. U.S.A. **106**, 17359 (2009).
[21] Y. Lan and G. A. Papoian, Phys. Rev. Lett. **98**, 228301 (2007).
[22] B. V. Adkar, B. Jana, and B. Bagchi, J. Phys. Chem. A **115**, 3691 (2011).
[23] W. Cleland, Biochim. Biophys. Acta **67**, 104 (1963).
[24] J. N. Onuchic, Z. Luthey-Schulten, and P. G. Wolynes, Annu. Rev. Phys. Chem. **48**, 545 (1997).
[25] C. Müller, G. Schlauderer, J. Reinstein, and G. E. Schulz, Structure **4**, 147 (1996).
[26] J. Ådén, A. Verma, A. Schug, and M. Wolf-Watz, J. Am. Chem. Soc. **134**, 16562 (2012).
[27] W.-T. Chu and J. Wang, Sci. Rep. **6**, 27808 (2016).
[28] K.-I. Okazaki, N. Koga, S. Takada, J. N. Onuchic, and P. G. Wolynes, Proc. Natl. Acad. Sci. U.S.A. **103**, 11844 (2006).
[29] K.-I. Okazaki and S. Takada, Proc. Natl. Acad. Sci. U.S.A. **105**, 11182 (2008).
[30] W. Li, W. Wang, and S. Takada, Proc. Natl. Acad. Sci. U.S.A. **111**, 10550 (2014).
[31] See Supplemental Material at http://link.aps.org/supplemental/10.1103/PhysRevLett.122.238102 for additional model description and discussion, which includes Refs. [32–60].
[32] W. Li, T. Terakawa, W. Wang, and S. Takada, Proc. Natl. Acad. Sci. U.S.A. **109**, 17789 (2012).

[33] D. M. Zuckerman, J. Phys. Chem. B **108**, 5127 (2004).
[34] P. Maragakis and M. Karplus, J. Mol. Biol. **352**, 807 (2005).
[35] Y.-G. Chen and G. Hummer, J. Am. Chem. Soc. **129**, 2414 (2007).
[36] M. Knott and R. B. Best, J. Chem. Phys. **140**, 175102 (2014).
[37] J. Reinstein, I. R. Vetter, I. Schlichting, P. Roesch, A. Wittinghofer, and R. S. Goody, Biochemistry **29**, 7440 (1990).
[38] E. Brunk and U. Rothlisberger, Chem. Rev. **115**, 6217 (2015).
[39] A. Washel and M. Levitt, J. Mol. Biol. **103**, 227 (1976).
[40] A. T. Carvalho, A. Barrozo, D. Doron, A. V. Kilshtain, D. T. Major, and S. C. L. Kamerlin, J. Mol. Graphics Modell. **54**, 62 (2014).
[41] M. Karplus, Proc. Natl. Acad. Sci. U.S.A. **107**, E71 (2010).
[42] M. Kovermann, J. Ådén, C. Grundström, A. E. Sauer-Eriksson, U. H. Sauer, and M. Wolf-Watz, Nat. Commun. **6**, 7644 (2015).
[43] O. Miyashita, J. N. Onuchic, and P. G. Wolynes, Proc. Natl. Acad. Sci. U.S.A. **100**, 12570 (2003).
[44] P. C. Whitford, S. Gosavi, and J. N. Onuchic, J. Biol. Chem. **283**, 2042 (2008).
[45] M. Wolf-Watz, V. Thai, K. Henzler-Wildman, G. Hadjipavlou, E. Z. Eisenmesser, and D. Kern, Nat. Struct. Mol. Biol. **11**, 945 (2004).
[46] M. Pirchi, G. Ziv, I. Riven, S. S. Cohen, N. Zohar, Y. Barak, and G. Haran, Nat. Commun. **2**, 493 (2011).
[47] A. C. Wallace, R. A. Laskowski, and J. M. Thornton, Protein Eng., Des. Sel. **8**, 127 (1995).
[48] S. Takada, R. Kanada, C. Tan, T. Terakawa, W. Li, and H. Kenzaki, Acc. Chem. Res. **48**, 3026 (2015).
[49] N.-V. Buchete and G. Hummer, J. Phys. Chem. B **112**, 6057 (2008).
[50] L. Martini, A. Kells, R. Covino, G. Hummer, N.-V. Buchete, and E. Rosta, Phys. Rev. X **7**, 031060 (2017).
[51] J.-H. Prinz, H. Wu, M. Sarich, B. Keller, M. Senne, M. Held, J. D. Chodera, C. Schütte, and F. Noé, J. Chem. Phys. **134**, 174105 (2011).
[52] W. Wang, S. Cao, L. Zhu, and X. Huang, WIREs Comput. Mol. Sci. **8**, e1343 (2018).
[53] D. A. Case, V. Babin, J. Berryman, R. Betz, Q. Cai, D. Cerutti, T. Cheatham III, T. Darden, R. Duke, H. Gohlke *et al.*, *Amber 14* (University of California, San Francisco, 2014).
[54] J. A. Maier, C. Martinez, K. Kasavajhala, L. Wickstrom, K. E. Hauser, and C. Simmerling, J. Chem. Theory Comput. **11**, 3696 (2015).
[55] W. L. Jorgensen, J. Chandrasekhar, J. D. Madura, R. W. Impey, and M. L. Klein, J. Chem. Phys. **79**, 926 (1983).
[56] K. L. Meagher, L. T. Redman, and H. A. Carlson, J. Comput. Chem. **24**, 1016 (2003).
[57] M. B. Berry and G. N. Phillips Jr., Proteins **32**, 276 (1998).
[58] T. Darden, D. York, and L. Pedersen, J. Chem. Phys. **98**, 10089 (1993).
[59] W. L. DeLano, *The PyMOL Molecular Graphics System* (DeLano Scientific, San Carlos, 2009).
[60] H. P. Lu, L. Xun, and X. S. Xie, Science **282**, 1877 (1998).
[61] B. Jana, B. V. Adkar, R. Biswas, and B. Bagchi, J. Chem. Phys. **134**, 035101 (2011).
[62] Y. Wang, L. Gan, E. Wang, and J. Wang, J. Chem. Theory Comput. **9**, 84 (2013).
[63] H. Yaginuma, S. Kawai, K. V. Tabata, K. Tomiyama, A. Kakizuka, T. Komatsuzaki, H. Noji, and H. Imamura, Sci. Rep. **4**, 6522 (2014).
[64] M. Kovermann, C. Grundström, A. E. Sauer-Eriksson, U. H. Sauer, and M. Wolf-Watz, Proc. Natl. Acad. Sci. U.S.A. **114**, 6298 (2017).
[65] A. Fersht, *Structure and Mechanism in Protein Science*, 2nd ed. (W. H. Freeman and Co., New York, 1999).
[66] A. Warshel, J. Biol. Chem. **273**, 27035 (1998).
[67] D. U. Ferreiro, E. A. Komives, and P. G. Wolynes, Q. Rev. Biophys. **47**, 285 (2014).
[68] W. Li, P. G. Wolynes, and S. Takada, Proc. Natl. Acad. Sci. U.S.A. **108**, 3504 (2011).
[69] H. Kenzaki, N. Koga, N. Hori, R. Kanada, W. Li, K.-I. Okazaki, X.-Q. Yao, and S. Takada, J. Chem. Theory Comput. **7**, 1979 (2011).